



## ZINC OXIDE AS A CORROSION INHIBITOR UPON MILD STEEL IN 0.5 M HCL SOLUTION



<sup>1</sup>Ogoru, S. O. and <sup>2</sup>Okewale, A. O.

Federal University of Petroleum Resources, Effurun Delta State, Nigeria

<sup>1,2</sup>Department of Chemical Engineering, P.M.B., 1221.

<sup>1</sup>[omas12118@gmail.com](mailto:omas12118@gmail.com), <sup>2</sup>[Okewale.akindele@fupre.edu.ng](mailto:Okewale.akindele@fupre.edu.ng).

Received: October 14, 2024 Accepted: December 28, 2024

**Abstract:** Corrosion remains a significant barrier to metal components' durability and structural integrity, especially under harsh conditions such as hydrochloric acid (HCl) exposure. This research investigates how varying concentrations of zinc oxide (ZnO) inhibitors—50, 100, 150, and 200 ppm—impact the corrosion rate of mild steel in 0.5M HCl at temperatures ranging from 30°C to 60°C. Electrochemical techniques, including potentiodynamic polarisation and linear sweep voltammetry (LSV) via open-circuit potential (OCP) measurements, were employed to evaluate the effectiveness of ZnO in reducing the corrosion rate. Results showed a notable reduction in corrosion rate as ZnO concentrations increased across all temperature conditions. Specifically, at 30°C, the corrosion rate of mild steel decreased by as much as 89.21% at the highest ZnO concentration, highlighting ZnO's efficacy in mitigating corrosion. Adding ZnO also led to higher polarisation resistance, suggesting enhanced corrosion resistance. OCP results showed a shift towards more positive potentials, indicating effective inhibition of both anodic and cathodic reactions. This suggests that ZnO promotes the formation of a protective layer on the steel surface, which reduces the overall corrosion process. The study demonstrates ZnO's potential as an effective corrosion inhibitor in aggressive environments. Its ability to reduce corrosion rates and increase polarisation resistance indicates promise for extending the lifespan of metallic structures in corrosive settings. Positive enthalpy values ( $\Delta H$ ) imply an endothermic adsorption process, while negative entropy values ( $\Delta S$ ) indicate a more structured arrangement of inhibitor molecules on the steel surface. Activation energy ranged from 9,972.41 J/mol without ZnO to 16,532.79 J/mol with ZnO, suggesting that the bond formation between ZnO and steel surface primarily involves physical adsorption.

**Keywords:** Corrosion, Electrochemical, Linear Sweep Voltammetry (LSV), ZnO, Corrosion Rate, Thermodynamics, Inhibitor.

### 1.0 Introduction

Corrosion is a pervasive and costly issue that impacts various industries, including manufacturing, infrastructure, and transportation. Low-carbon steel, in particular, is highly susceptible to degradation, especially in aggressive environments. The detrimental effects of corrosion on the durability and structural integrity of steel assets have driven extensive research into effective corrosion inhibitors. In recent years, nanotechnology has emerged as a promising area for corrosion control due to the unique properties of nanoparticles. Among these, zinc oxide (ZnO) has gained significant interest for its potential in corrosion prevention. Researchers are examining ZnO particles as innovative inhibitors for mild steel in aggressive environments, leveraging ZnO's unique physicochemical properties. Notably, ZnO's photocatalytic activity, large surface area, and stability make it a strong candidate for corrosion protection (Sahoo et al, 2018).

Utilising inhibitors is one of the most effective strategies to counteract corrosion in hostile conditions. This approach may involve forming a more resilient coating or using adsorptive inhibitors to prevent damaging ions from attaching to metal surfaces (Elmaghaby et al, 2009). This study's findings support advancements in corrosion inhibitors, aiming to improve the durability and lifespan of low-carbon steel structures in aggressive settings. Additionally, these inhibitors offer an environmentally friendly alternative, reducing dependence on hazardous chemicals while effectively combating corrosion. By evaluating zinc oxide as a corrosion inhibitor for mild steel

in HCl solutions, this research contributes to the field of corrosion science, establishing a foundation for novel corrosion prevention methods. The study examines ZnO effectiveness as a corrosion inhibitor on mild steel surfaces in aggressive media using a range of electrochemical techniques.

### 2.1 Materials and Methods

#### 2.1.1 Material

The materials used in this experimental study included mild steel (coupon), zinc oxide (ZnO), concentrated hydrochloric acid (HCl) at 0.5M, ethanol, demineralised water, and acetone. All chemicals were obtained from Sigma-Aldrich and were of analytical grade.

#### 2.1.2 Instruments and Apparatus

The apparatus utilised included conical flasks, beakers, measuring cylinders, a hacksaw, a digital weighing balance, a laboratory oven, a water bath, a metal file, emery cloth, a brush, thread, and a mild steel coupon sample. Laboratory instruments involved a Gallenkamp laboratory oven, a DZKW-S-4 water bath, an AUTOLAB potentiostat/galvanostat (PGSTAT 101), a PGW 753i weighing balance, a personal computer, and AutoLab ANOVA software.

### 2.2 Methods

#### 2.2.1 Sample Preparation and Pre-treatment

Zinc oxide and mild steel coupons were procured from certified chemical and metal suppliers in Effurun, Delta State, Nigeria. The mild steel coupons, measuring 40mm x

20mm x 2mm, were fabricated from mild steel sheets. To prepare the specimens, the coupons were descaled using a wire brush, then polished to a smooth finish with 120-150 grit abrasive paper, cleaned with acetone, air-dried, and stored in an anhydrous environment until use.

### 2.2.2 Electrochemical Analysis of the Corrosion Inhibition Process

The mild steel sample was polished with various grades of abrasive paper to achieve a smooth surface and then degreased with acetone. The electrochemical experiment was conducted in a 0.5M HCl medium within a 100 mL glass cell, following ASTM G3/G102 standards for electrochemical measurements. The AUTOLAB potentiostat/galvanostat (PGSTAT 101) was employed, featuring a three-electrode setup: the mild steel sample as the working electrode (WE), a graphite rod as the counter electrode, and a glass-body calomel electrode (Onesil brand) containing Ag/AgCl (3M KCl) as the reference electrode. The working electrode was attached to a copper wire and mounted on epoxy resin, with 1.5 cm<sup>2</sup> of its surface exposed to the acidic solution. At the same time, 25 mm of the graphite rod was immersed in the electrolyte.

The experiment was conducted at temperatures of 30 °C, 40 °C, 50 °C, and 60 °C in a glass cell holding 100 mL of electrolyte solution. Linear sweep voltammetry (LSV) was configured using ANOVA 2.1.2 software, with an initial potential of -1.5 V and a final potential of +1.5 V relative to the open-circuit potential (OCP), at a scan rate of 0.001 V s<sup>-1</sup>. Each test was run for 60 minutes and repeated thrice for similar specimens to ensure consistent results. Based on Tafel extrapolation of the anodic and cathodic branches, the corrosion potential (E<sub>corr</sub>), corrosion current density (J<sub>corr</sub>), anodic slope (ba), and cathodic slope (bc) were determined (Fouda et al, 2021).

**Table 1: Elemental makeup of ZnO**

Elements	ZnO	Cl	SO <sub>4</sub>	NO <sub>3</sub>	Mn	Fe	As	Pb
% Conc.	99.0	<0.001	<0.01	<0.003	<0.0005	<0.0005	<0.0005	<0.005

### 3.2 Electrochemical Analysis of Corrosion-Inhibited Steel Samples in 0.5M HCl

Table 2 provides a detailed analysis of parameters from the electrochemical study, including electrochemical potential (E<sub>corr</sub>), current density (J<sub>corr</sub>), corrosion rate, and polarisation resistance across various ZnO concentrations in HCl. The data consistently show that higher ZnO concentrations are linked to reduced corrosion rates, demonstrating ZnO's efficacy in forming protective layers of overactive corrosive regions on the steel surface. At 30°C, the corrosion rate significantly decreased by 2.12 mm/yr, correlating with a 66.1% reduction in material loss.

The Tafel plot data in Table 2 supports these findings, showing that as ZnO concentration increased (Popoola and Fayomi, 2011), corrosion rates dropped. Moreover, current density values rose alongside ZnO concentration, reflecting

The corrosion rate (CR) and polarisation resistance (PR) were calculated using equations (1) and (2), while the ZnO inhibitor's effectiveness was evaluated using equation (3).

$$CR = (0.00327 \times 5 \frac{J_{corr} \times w_{eq}}{\rho})$$

(1)

Where j<sub>corr</sub> represents the corrosion current flow density per square centimetre, ρ is the metal coupon density in grams per cubic centimetre, and w<sub>eq</sub> is the equivalent weight of the coupon in grams. The oxidation rate was calculated in millimetres per year.

$$PR = 2.303 \frac{abc}{J_{corr}(ba+bc)}$$

(2)

$$\% IE = \frac{i_{0corr} - i_{corr}}{i_{corr}} \times 100$$

(3)

Where i<sub>0corr</sub> and i<sub>corr</sub> correspond to the dearth and occurrence of corrosion current flow density of the ZnO inhibitor, respectively.

## 3. Results and Discussion

### 3.1 Chemical Composition of ZnO Particles

Zinc oxide (ZnO) is primarily comprised of zinc (Zn) and oxygen (O) atoms arranged in a stable crystalline structure, with trace amounts of other elements (Almosawi et al, 2021). Table 1 outlines ZnO's elemental composition. Zinc, a transition metal, forms the core of these nano-scale particles, lending strength and specific physical characteristics. The oxygen atoms complement zinc, creating the ZnO compound with chemical bonds. This crystalline arrangement imparts distinctive properties to ZnO, including semiconductor behaviour, photocatalytic activity, and biocompatibility, making it valuable across diverse technological and biomedical fields (Mahamuni et al, 2019).

ZnO's effectiveness in reducing the susceptibility of active sites to chloride ions within the HCl solution. Typically, higher temperatures accelerate corrosion rates due to faster electrochemical reactions, but the presence of ZnO yielded the opposite trend. ZnO showed improved adsorption and surface coverage at elevated temperatures, forming a more robust protective film that limited corrosive agent penetration, thereby reducing corrosion despite the increased reactivity at higher temperatures (Sully, 2019). Enhanced polarization resistance with higher ZnO concentrations further demonstrates ZnO role in corrosion protection, indicating the ability of ZnO particles to bond to the steel surface and inhibit electrochemical processes responsible for corrosion (Dong et al, 2018). This led to more effective corrosion inhibition and longer metal lifespan.

**Table 2: Parameters from Tafel Chart of sample steel within aggressive medium between 30 °C – 60 °C**

Temperature	Samples	E <sub>CORR</sub> (V)	J <sub>CORR</sub> (A/cm <sup>2</sup> )	C <sub>R</sub> (mm/yr)	P <sub>R</sub> (Ω)
30°C	BLANK	-0.25	1.14×10 <sup>-04</sup>	6.25	4.77×10 <sup>1</sup>
	50ppm	-0.348	1.43×10 <sup>-04</sup>	5.01	5.94×10 <sup>2</sup>
	100ppm	-0.46	1.53×10 <sup>-04</sup>	4.79	1.68×10 <sup>2</sup>
	150ppm	-0.33	2.54×10 <sup>-04</sup>	4.77	1.01×10 <sup>2</sup>
	200ppm	-0.362	2.81×10 <sup>-04</sup>	4.13	3.19×10 <sup>2</sup>
40°C	BLANK	-0.388	9.18×10 <sup>-05</sup>	7.4	1.45×10 <sup>2</sup>
	50ppm	-0.412	1.21×10 <sup>-04</sup>	7.05	1.24×10 <sup>2</sup>
	100ppm	-0.44	2.32×10 <sup>-04</sup>	6.84	8.01×10 <sup>2</sup>
	150ppm	-0.33	2.54×10 <sup>-04</sup>	6.22	1.01×10 <sup>2</sup>
	200ppm	-0.346	2.81×10 <sup>-04</sup>	5.89	3.19×10 <sup>2</sup>
50°C	BLANK	-0.324	9.44×10 <sup>-05</sup>	7.25	3.37×10 <sup>1</sup>
	50ppm	-0.388	1.77×10 <sup>-04</sup>	7.01	1.45×10 <sup>2</sup>
	100ppm	-0.427	2.61×10 <sup>-04</sup>	6.72	3.38×10 <sup>1</sup>
	150ppm	-0.432	2.66×10 <sup>-04</sup>	6.11	1.30×10 <sup>2</sup>
	200ppm	-0.462	3.80×10 <sup>-03</sup>	6.06	2.29×10 <sup>2</sup>
60°C	BLANK	-0.465	8.02×10 <sup>-04</sup>	9.29	8.02×10 <sup>-3</sup>
	50ppm	-0.478	1.44×10 <sup>-03</sup>	9.01	1.66×10 <sup>1</sup>
	100ppm	-0.492	1.73×10 <sup>-03</sup>	8.54	1.68×10 <sup>2</sup>
	150ppm	-0.502	2.34×10 <sup>-03</sup>	8.11	1.01×10 <sup>2</sup>
	200ppm	-0.512	2.61×10 <sup>-03</sup>	7.84	1.19×10 <sup>2</sup>

### 3.3 Open Circuit Potential Analysis of Mild Steel Samples

The open-circuit potential (OCP) reflects the electrochemical corrosion characteristics of the steel samples with and without ZnO. Figures 1 to 4 illustrate the potential (V) over time (secs) at ZnO concentrations across temperatures from 30°C to 60°C. Generally, mild steel samples in ZnO-containing solutions shifted gradually towards more positive potential values. The positive shift indicates a more substantial inhibitory effect on the anodic reactions. The potential rose to more positive values when ZnO was added than samples in ZnO-free solutions. In Figure 1, the ZnO-containing samples initially ranged from -0.15 to -0.05 V within the first 20 seconds, similar to trends observed in Figures 3 and 5. Notably, both the ZnO and ZnO-free samples displayed nearly linear potential-time curves, indicating that a stable state potential had been achieved. As the temperature increased, potential values became more negative over time, reflecting higher aggression in the oxidative environment with prolonged immersion (Gupta et al, 2017).

Figures 2, 4, 6, and 8 illustrate the anodic and cathodic reactions of mild steel in the acidic medium at varying ZnO concentrations and temperatures. The Tafel plots show a

general decrease in both anodic and cathodic reaction rates with increasing ZnO concentration, suggesting ZnO's multifunctional role as a corrosion inhibitor in 0.5M HCl (Kumar et al, 2011; Nwosu and Amusat, 2021).

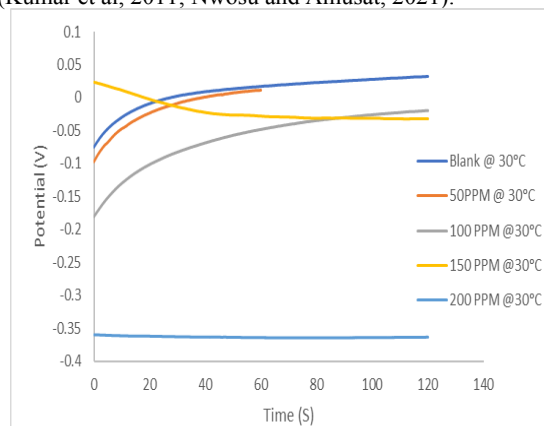


**Figure 1: OCP Plot of samples within 0.5M HCl at 30 °C temperature**

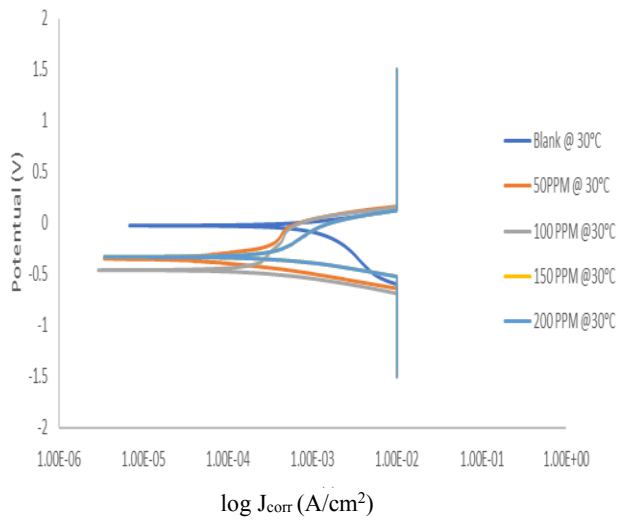


Figure 2: Tafel dipole formation of sample at 30°C from LSV.

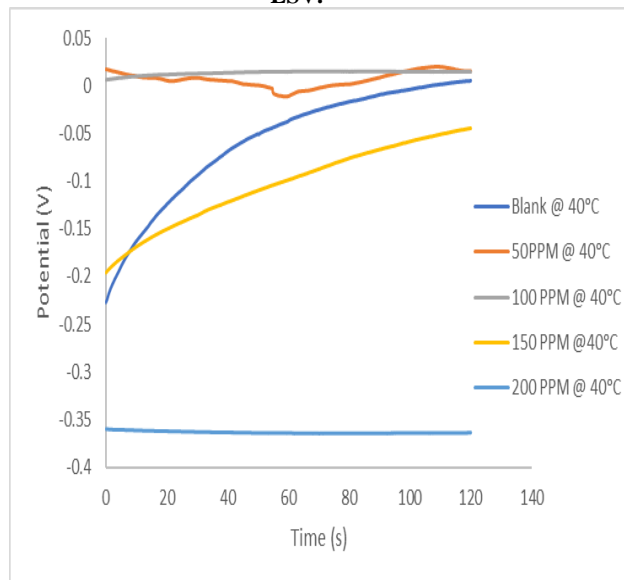


Figure 3: OCP Plot of sample within 0.5M HCl at 40 °C temperature

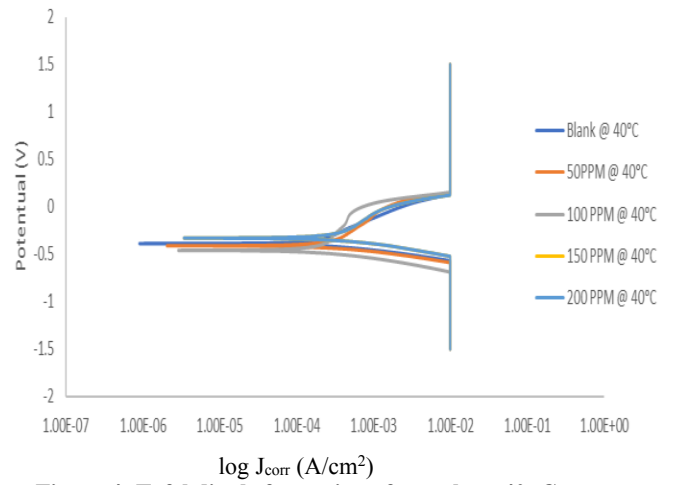


Figure 4: Tafel dipole formation of sample at 40 °C from LSV

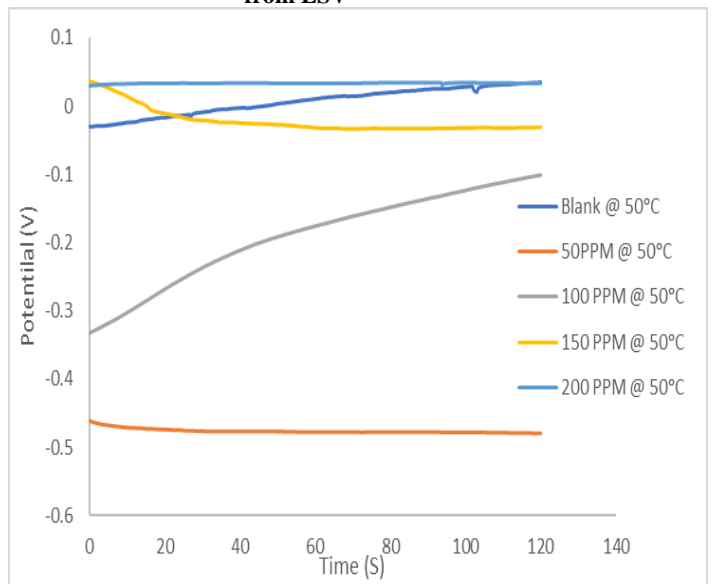


Figure 5: OCP Plot of sample within 0.5M at 50 °C temperature

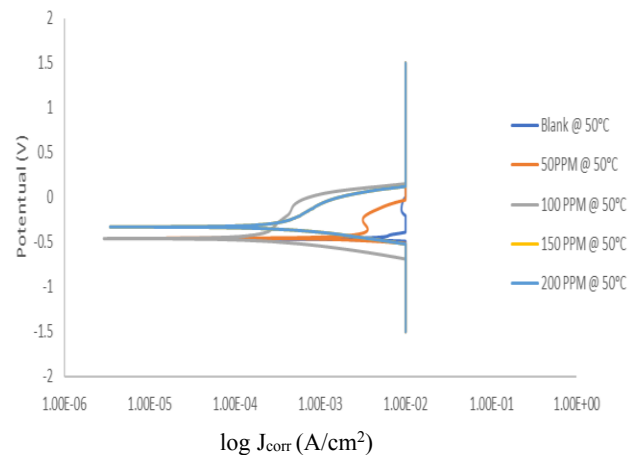


Figure 6: Tafel dipole formation of sample at 50 °C from LSV

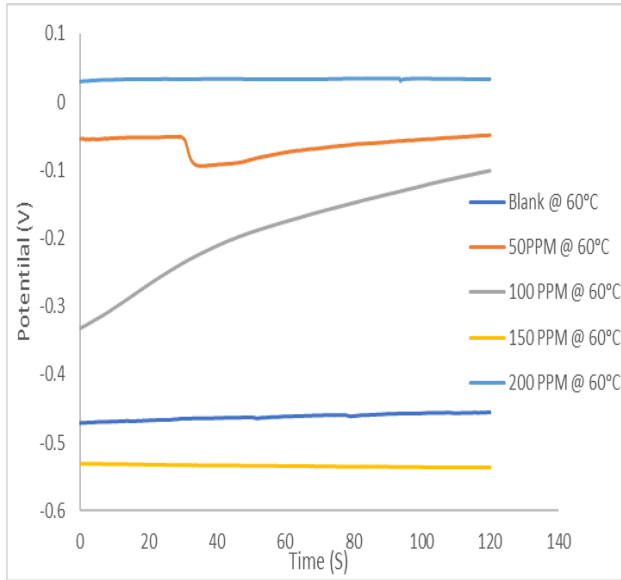


Figure 7: OCP Plot of sample at 0.5M of HCl at 60 °C temperature

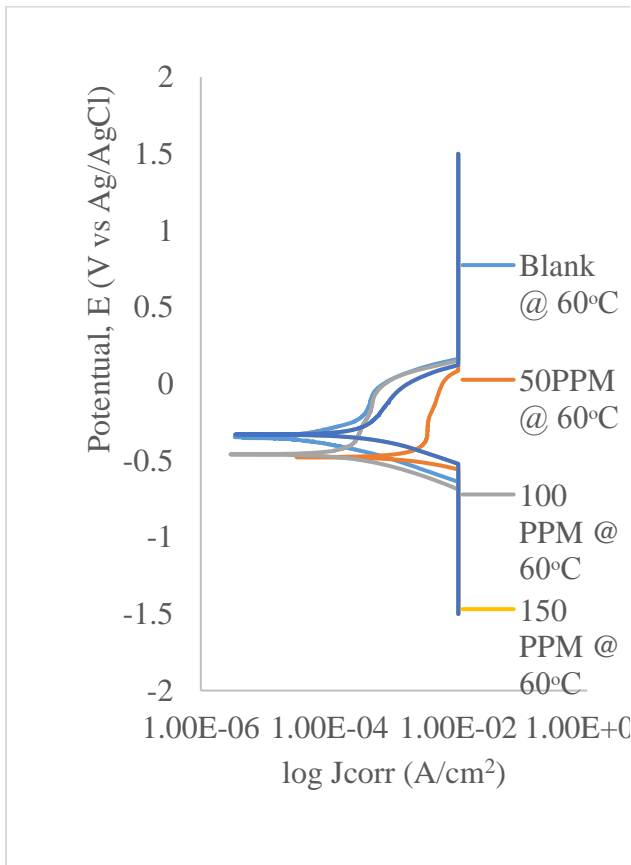


Figure 8: Tafel dipole formation of sample at 60 °C

from LSV.

### 3.4 Effect of Temperature on Corrosion Rate with ZnO Inhibition

As illustrated in Figure 9, the corrosion rate decreased consistently with increasing ZnO concentration across temperatures from 30°C to 60°C. Although inhibition strength rose with increased ZnO concentration, the corrosion rate increased slightly with higher temperatures. This trend may be attributed to the heightened reactivity of chloride ions (Cl<sup>-</sup>) within HCl at elevated temperatures, allowing for a more aggressive attack on the mild steel surface (Negm et al, 2010).

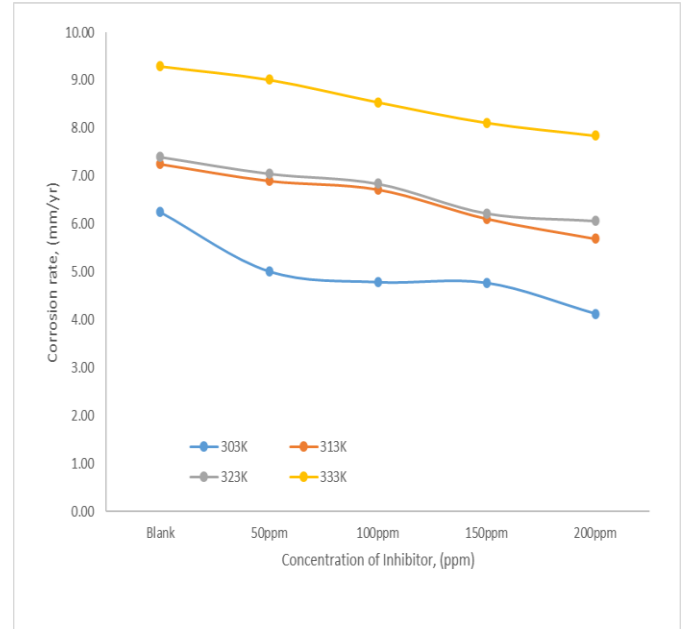


Figure 9: Temperature effect on ZnO concentration inhibition in 0.5M HCl.

### 3.5 Activation Parameters for the Corrosion Process

Temperature changes influence all electrochemical systems, affecting adsorption and kinetic parameters, including activation energy and enthalpy. Thermal energy (enthalpy) accounts for a system's total internal energy, while entropy reflects the degree of disorder. Using Arrhenius plots, which plot the natural logarithm of corrosion current density (ln J<sub>CORR</sub>) against the reciprocal of temperature (1/T), insight into activation energy can be obtained as described by equation (4).

$$\ln J_{CORR} = \ln \lambda - \frac{E_a}{2.303RT} \quad (4)$$

In Figure 10, the Arrhenius plot reveals a nearly linear relationship, allowing assessment of activation energy (E<sub>a</sub>) and pre-exponential factor (λ) based on the slope and intercept of the linear plot.

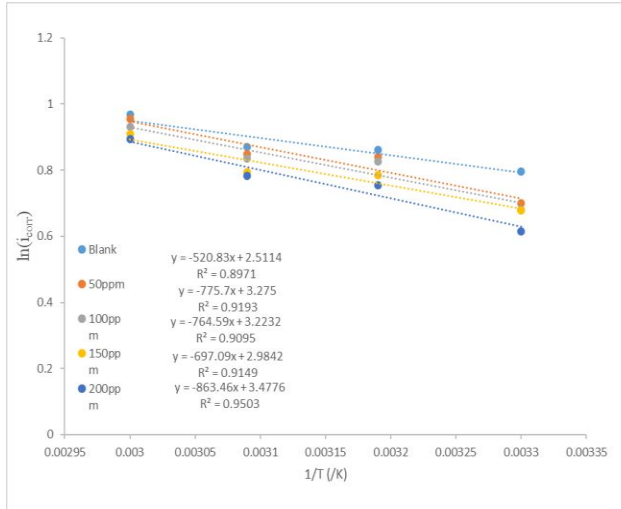


Figure 10: Chart of  $\ln(J_{corr})$  against  $1/T$  in 0.5M HCl.

Table 3 presents activation energy values ranging from 9,972.41 J/mol in the absence of ZnO to 16,532.79 J/mol

Table 3: Arrhenius Parameters of Sample

Acid Concentration	Samples	$E_A$ (J/mol)	$\lambda$
0.5 M	Blank	9,972.41	6.827
	50ppm	14,852.44	8.902
	100ppm	14,639.71	8.762
	150ppm	13,347.28	8.112
	200ppm	16,532.79	9.453

### 3.6 Thermodynamic Parameters for Adsorption

Thermodynamic parameters for enthalpy and entropy of adsorption on mild steel in both inhibited and uninhibited HCl solutions were determined using equation (5).

$$\ln\left(\frac{j_{corr}}{T}\right) = \ln\left(\frac{R}{Nh}\right) + \frac{\Delta S_{ads}}{2.303R} - \frac{\Delta H_{ads}}{2.303RT} \quad (5)$$

The plot of  $\ln(j_{corr}/T)$  against  $1/T$ , shown in Figure 11, yielded a linear trend from which enthalpy ( $\Delta H$ ) and entropy ( $\Delta S^\circ$ ) values were derived (Table 4). Positive  $\Delta H$  values indicate that the adsorption process is endothermic, while negative  $\Delta S^\circ$  values suggest a more orderly arrangement of ZnO molecules on the steel surface. The negative entropy values imply that the products formed during adsorption possess lower entropy than the initial reactants, indicating a reduction in disorder as the system transitions from reactants to an activated state (Sudhish and Eno, 2011; Akinbulumo et al, 2020). The average discrepancy between activation energy and enthalpy was calculated to be 2.613 kJ/mol, aligning with the product of the gas constant ( $R$ ) and the average temperature ( $T$ ), consistent with findings from prior studies (Noor, 2007; Noor, 2009). This outcome supports the idea that the corrosion process is a unimolecular reaction involving the release of hydrogen gas.

with a ZnO concentration of 200 ppm. Higher activation energy values with ZnO indicate that the corrosion process slowed when ZnO was present, suggesting the ZnO inhibitor raised the energy barrier for corrosion reactions. The observed activation energy values, lower than the 80,000 J/mol threshold for chemisorption (Eddy et al, 2009), support the conclusion that ZnO adsorption on the steel surface is primarily a physisorption process (Miralrio and Vazquez, 2020; Qiang et al, 2021).

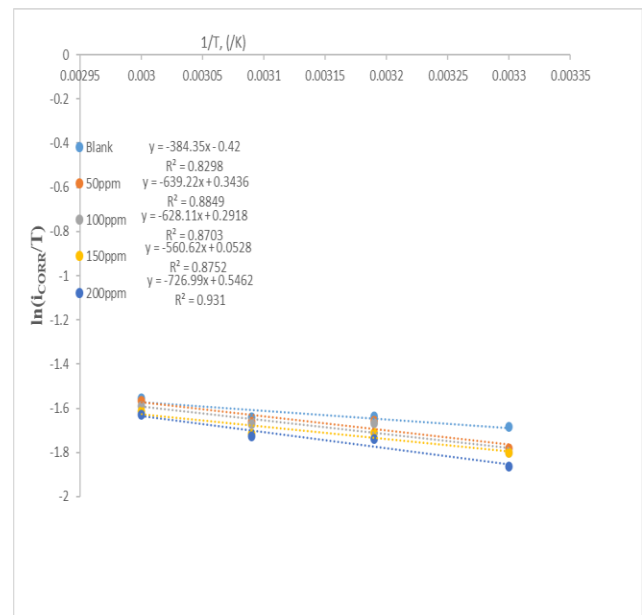


Figure 11: Chart of  $\ln(j_{corr}T^{-1})$  against  $T^{-1}$  within 0.5M HCl.

**Table 4: Thermodynamics of Adsorption Parameters of Sample in 0.5M HCl**

Acid Concentrations	Samples	$\Delta H_{Ads}$ (J/mol)	$\Delta S_{Ads}$ (J/mol)	$E_a - \Delta H_{Ads}$ (J/mol)
0.5 M	Blank	7,359.20	-489.02	2,613.21
	50ppm	12,239.24	-474.39	2,613.20
	100ppm	12,026.57	-475.39	2,613.14
	150ppm	10,734.27	-479.96	2,613.28
	200ppm	13,919.78	-470.52	2,613.01

#### 4 Conclusion

Evaluation of mild steel corrosion behaviour in 0.5 M HCl with ZnO as inhibitor was carried out using electrochemical method. The results showed that an increase in ZnO inhibitor concentrations significantly reduced corrosion rates across all the tested temperatures.

Elevated temperatures intensified the corrosion rate, but ZnO achieved 89.21% reduction in corrosion at the highest concentration tested, indicating its potential for mitigating metal degradation. The thermodynamic parameters derived in this study show that the adsorption of ZnO onto the mild steel surface is both orderly and endothermic. Analysis of polarisation plots and open-circuit potential (OCP) measurements demonstrated a shift toward more positive potentials with the presence of ZnO, this indicate the formation of a protective layer on the steel surface. This suggests that ZnO functions as a mixed-type inhibitor, enhancing adsorption and film formation over the steel surface, thereby increasing corrosion resistance as ZnO concentration rises.

#### References

Akinbulumo, O. S. S., Odejebi, O. J., and Odekanle, E. L., (2020), thermodynamics and adsorption study of the corrosion inhibition of mild steel by Euphorbia heterophylla L extract in 1.5 M HCl, *Results in materials*, 5, 100074

Al-Mosawi, B. T. S., Sabri, M. M., and Ahmed, M. A. (2021). Synergistic effect of ZnO nanoparticles with organic compound as corrosion inhibition. *International Journal of Low-Carbon Technologies*, 16(2), 429–435.

Dong, Y., Jiang, B., Xu Det, Jiang, Chengying, Qi Li. and Tingye Gu, (2018), Severe microbiologically influenced corrosion of S32654 super austenitic stainless steel by acid producing bacterium *Acidithiobacillus caldus* SM-1. *Bioelectrochemistry*. 123: 34–44.

Eddy, O. N., Odomelam, A. S., and Odionge, O. A., (2009), Ethanol extract of musa species peels as a green corrosion inhibitor for mild steel: Kinetics, adsorption and thermodynamic considerations, *Electronic Journal of Environmental, Agricultural and Food Chemistry*, 8(4), 243–255.

El Maghraby, A. A., (2009). Corrosion Inhibition of Aluminium in Hydrochloric Acid Solution using Potassium Iodate Inhibitor". *The Open Corrosion Journal*, 2, 189-196.

Fouda, A. E. A. S., El-Gharkawy, E. S., Ramadan, H., and El-Hossiany, A. (2021). Corrosion resistance of mild steel in hydrochloric acid solutions by clinopodium acinos as a green inhibitor. *Biointerface Research in Applied Chemistry*, 11(2). <https://doi.org/10.33263/BRIAC112.97869803>

Gupta, R. K., Malviya, M., Verma, C., and Quarishi, M. A. (2017). Aminoazobenzene and diaminoazobenzene functionalized graphene oxides as novel class of corrosion inhibitors for mild steel: experimental and DFT studies. *Master Chem Phys* 198, 360-373.

Kumar, K. P.V., Pillai, M. S. N., and Thusnavis, R., (2011), Seed extract of Psidium guajava as ecofriendly corrosion inhibitor for

carbon steel in hydrochloric acid medium, *Mat Sci Techno*. 2011, 27:1143-1149, [https://doi.org/10.1016/S1005-0302\(12\)60010-3](https://doi.org/10.1016/S1005-0302(12)60010-3).

Mahamuni, P. P., Patil, P. M., Dhanavade, M. J., Badiger, M. V., Shadija, P. G., Lokhande, A. C., and Bohara, R. A. (2019). Synthesis and characterization of zinc oxide nanoparticles by using polyol chemistry for their antimicrobial and antibiofilm activity. *Biochemistry and Biophysics Reports*, 17(September 2018), 71–80. <https://doi.org/10.1016/j.bbrep.2018.11.007>

Miralrio, A., & Vázquez, A. E. (2020). Plant extracts as green corrosion inhibitors for different metal surfaces and corrosive media: A review. *Processes*, 8(8). <https://doi.org/10.3390/PR8080942>

Negm, N. A., Al Sabagh, A. M., Migahed, M. A., Bary, H. A., and El Din, H. M. (2010). Effectiveness of some diquaternary ammonium surfactants as corrosion inhibitors for carbon steel in 0.5 M HCl solution. *Corrosion Science*, 52(6), 2122-2132.

Noor, E. A., (2007), temperature effects on the corrosion inhibition of mild steel in acidic solutions by aqueous extract of fenu Greek leaves, *International journal of electrochemical science*, 3, 996-1017.

Noor, E. A., (2009), Potential of aqueous extract of hibiscus sabdariffa leaves for inhibiting the corrosion of aluminum in alkaline solutions, *Journal applied electrochemical*, 39, 1465-1475.

Nwosu, J. F.O., and Amusat, S. O., (2021), Corrosion Inhibition of Mild Steel Using Parinari polyandra Leave Extracts in Diluted Hydrochloric Acids *Portugaliae Electrochimica Acta* 39. 431- 449.

Popoola, A. P. I., and Fayomi, O. S. I. (2011). ZnO as corrosion inhibitor for dissolution of zinc electrodeposited mild steel in varying HCl concentration. *International Journal of the Physical Sciences*, 6, 2447-2454.

Qiang, Y., Guo, L., Li, H., and Lan, X. (2021). Fabrication of environmentally friendly Losartan potassium film for corrosion inhibition of mild steel in HCl medium. *Chemical Engineering Journal*, 406. <https://doi.org/10.1016/j.cej.2020.126863>

Sahoo, P. K., Bano S., Mohamed A.P., Dey A., Pati R.K., Mohanta K., and Panigrahi S. (2018). Zinc Oxide: A Promising Multifunctional Candidate for Nanobiotechnology Applications. *Frontiers in Microbiology*, 9, 1211. doi: 10.3389/fmicb.2018.01211.

Sudhish, K. S., and Eno, E. E., (2011), corrosion inhibition adsorption behaviour and thermodynamics properties of streptomycin on mild steel in hydrochloric acid medium, *International journal of electrochemical science*, 3277-3291.

Sully, R. J., (2019), Future Frontiers in Corrosion Science and Engineering, Part III: The Next Leap Ahead in Corrosion Control May Be Enabled by Data Analytics and Artificial Intelligence, *Corrosion journal.org*, volume 75 (12), 1395 – 1397.